Supporting Information for

Differential influence of molybdenum disulfide at the nanometer and micron scales in the intestinal metabolome and microbiome of mice

Bing Wu↓, Ling Chen, Xiaomei Wu, Hui Hou, Zhizhi Wang, Su Liu

State Key Laboratory of Pollution Control and Resource Reuse, School of the Environment, Nanjing University, Nanjing, 210023, P.R. China

↓ Corresponding author: Email: bwu@nju.edu.cn

Address: 163 Xianlin Avenue, Nanjing, 210023, P.R. China

Table S1 Primers and conditions used in quantitative real-time PCR analysis

Gene		Sequence (5'-3')
β-actin	*F*	GTATGACTCCACTCACGGCAAA
	R	GGTCTCGCTCCTGGAAGATG
TNFa	*F*	AGCCCACGTCGTAGCAAACCAC
	R	ACACCCATTCCCTTCACAGAGC
MCP-1	*F*	AAAAACCTGGATCGGAACCAA
	R	CGGGTCAACTTCACATTCAAAG

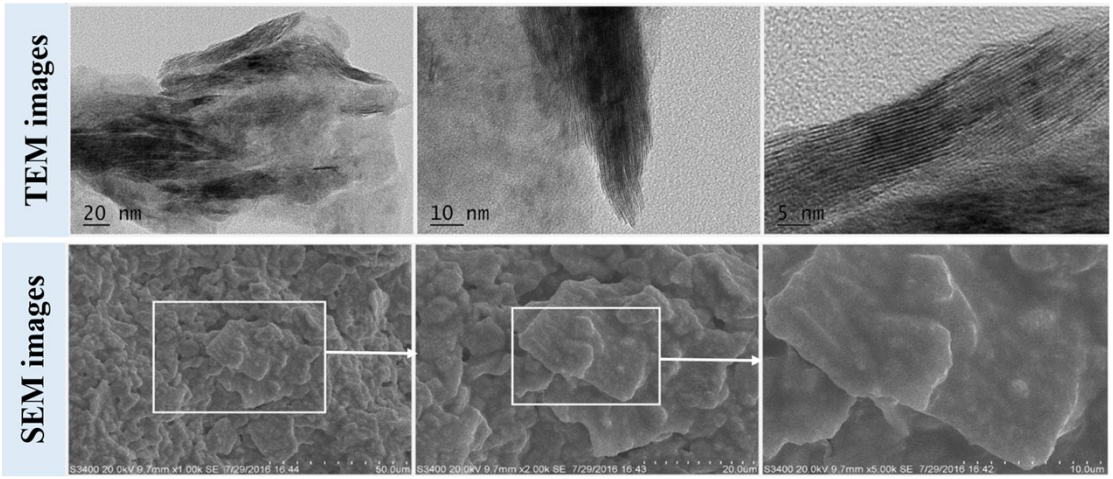

Figure S1 TEM and SEM images of the nano-MoS_2 used in this study.

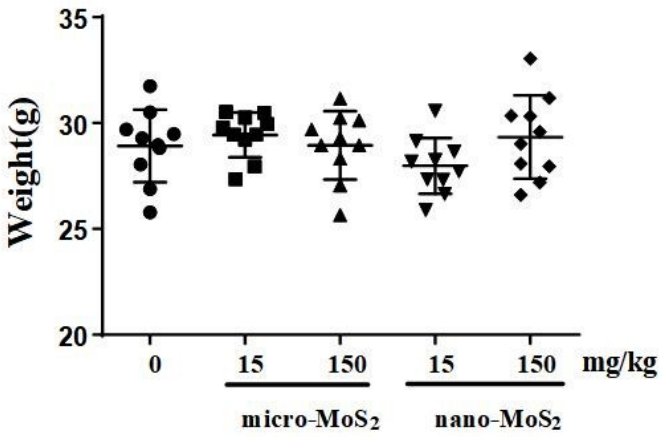

Figure S2 The body weight of the mice after 90-day exposure of nano- and micro-MoS_2. Ten mice were used in each group.

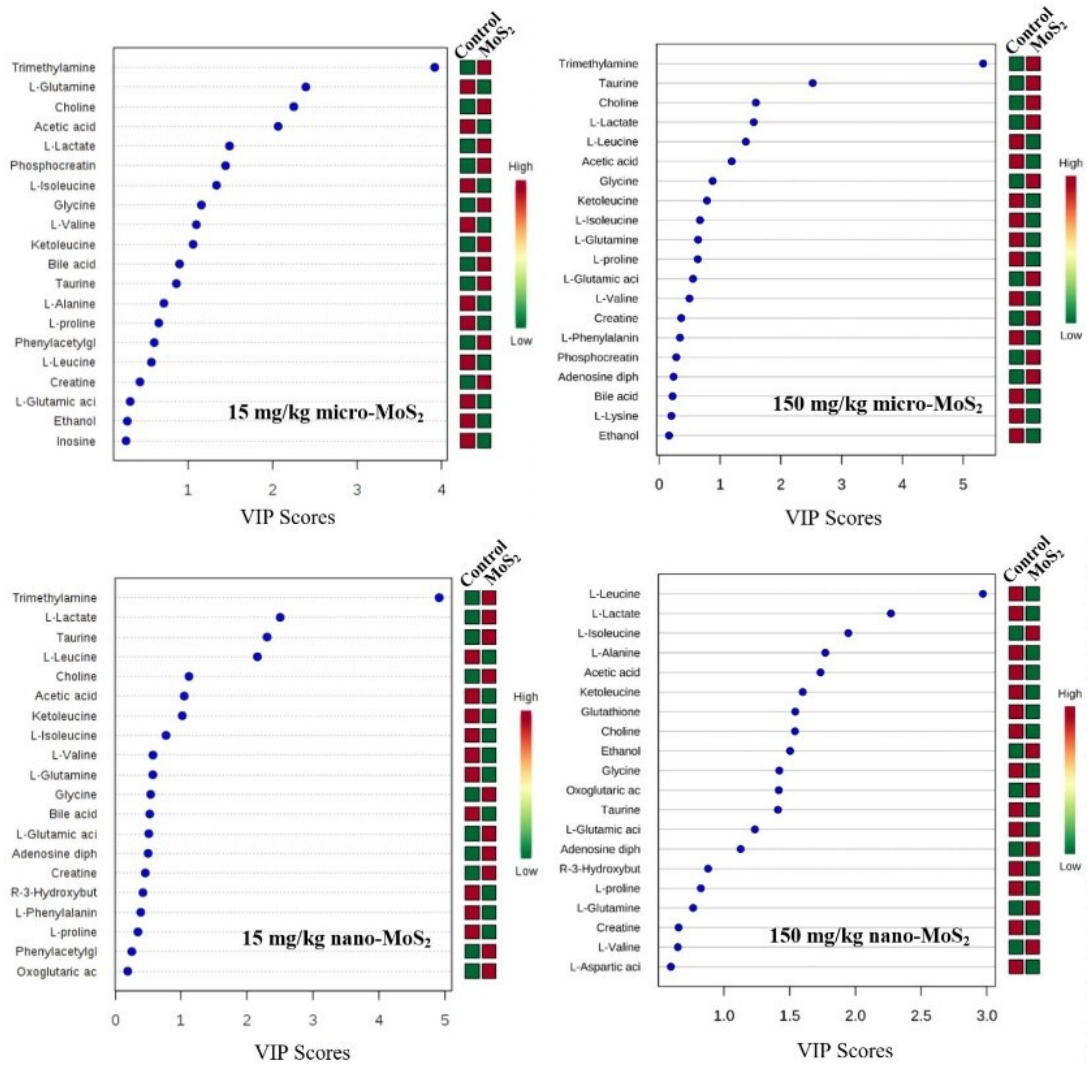

(A)

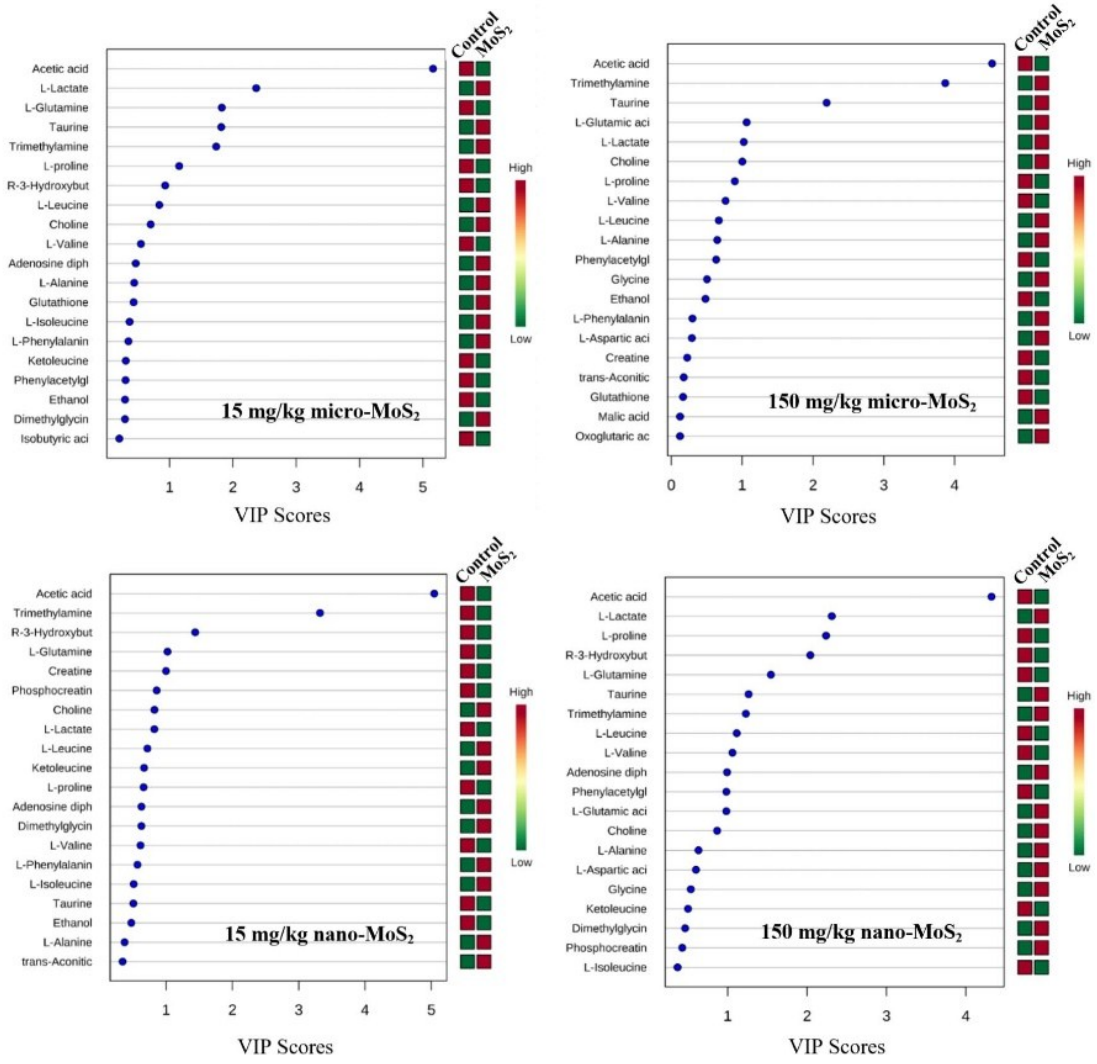

(B)

Figure S3 Metabolic profiles in the intestine after nano-MoS_2 and micro-MoS_2 exposure. (A) Small intestine; (B) Large intestine. A total of 20 metabolites were identified based on the cumulative variable importance in the projection (VIP) value of each metabolite, which was determined using the VIP analysis of MetaboAnalyst 3.0.

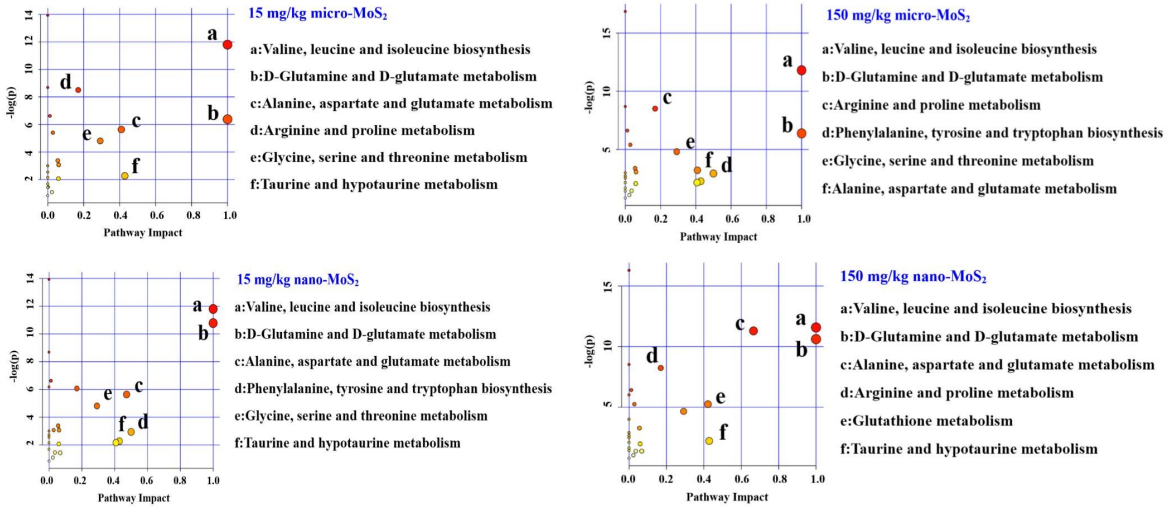

(A)

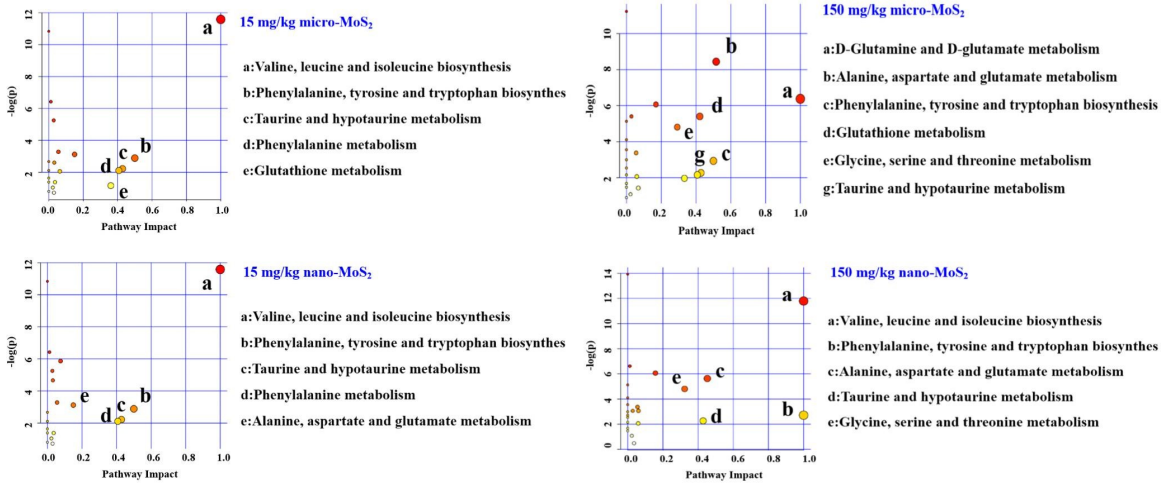

(B)

Figure S4 Influence of nano-MoS_2 and micro-MoS_2 on the metabolic pathways in the small and large intestine of mice. (A) Small intestine; (B) Large intestine. The metabolic pathways were determined using MetaboAnalyst 3.0

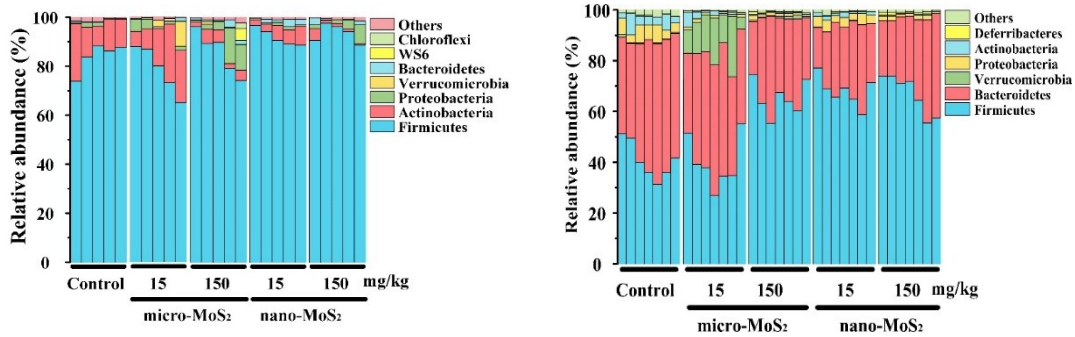

(A) (B)

Figure S5 Influence of nano-MoS_2 and micro-MoS_2 on the intestinal microbial community of mice at the phylum levels. (A) Small intestine; (B) Large intestine.

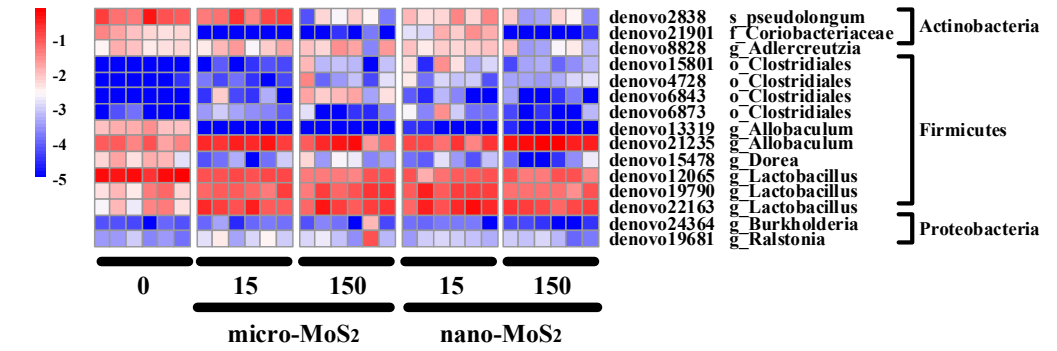

(A)

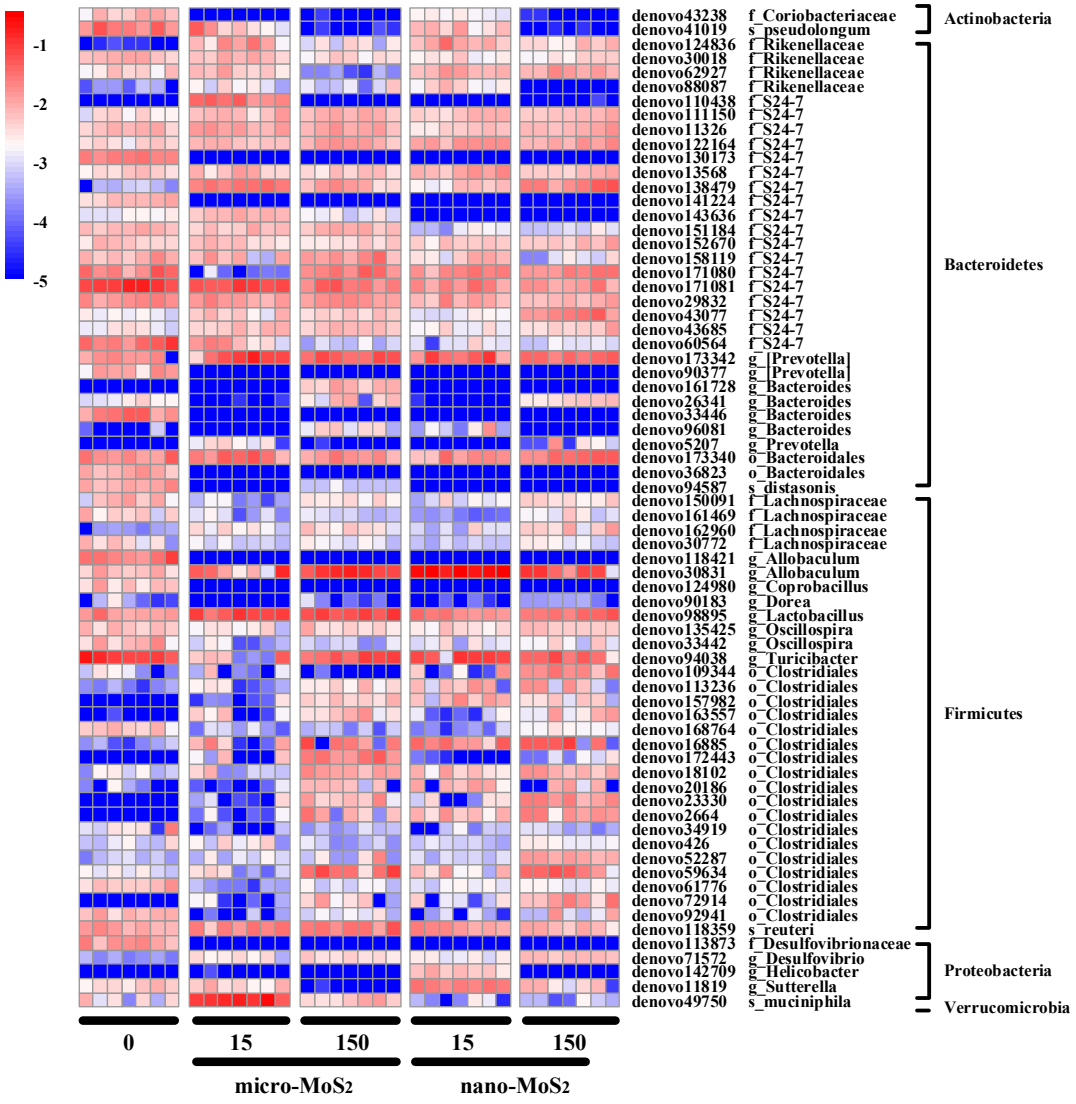

(B)

Figure S6 Comparison of the abundance of significantly altered OTUs in the intestine after nano- MoS_2 and micro-MoS_2 exposure. (A) OTUs in the small intestine; (B) OTUs in the large intestine. The heatmaps were constructed using the R language.

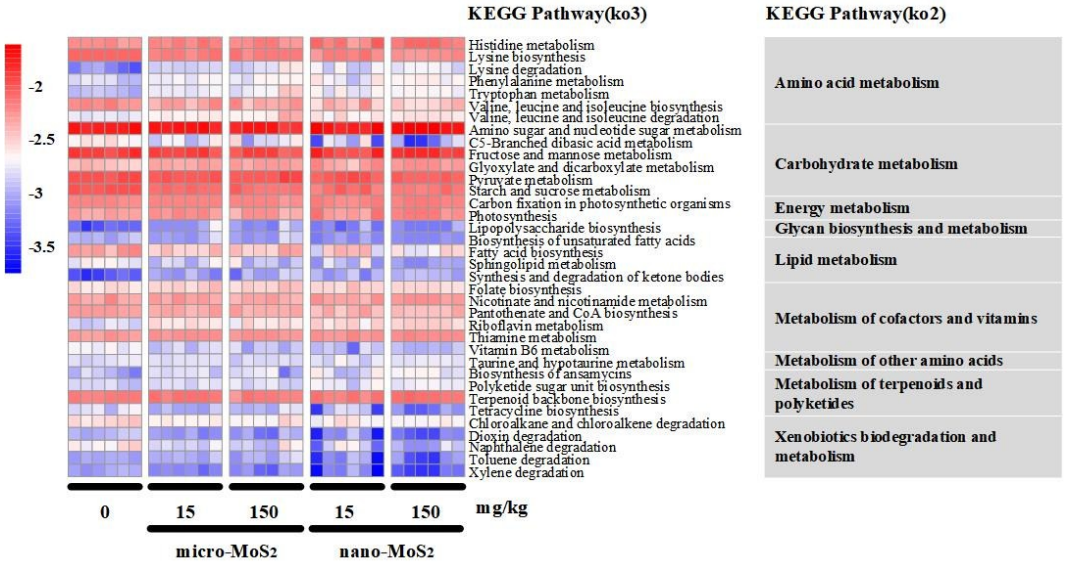

(A)

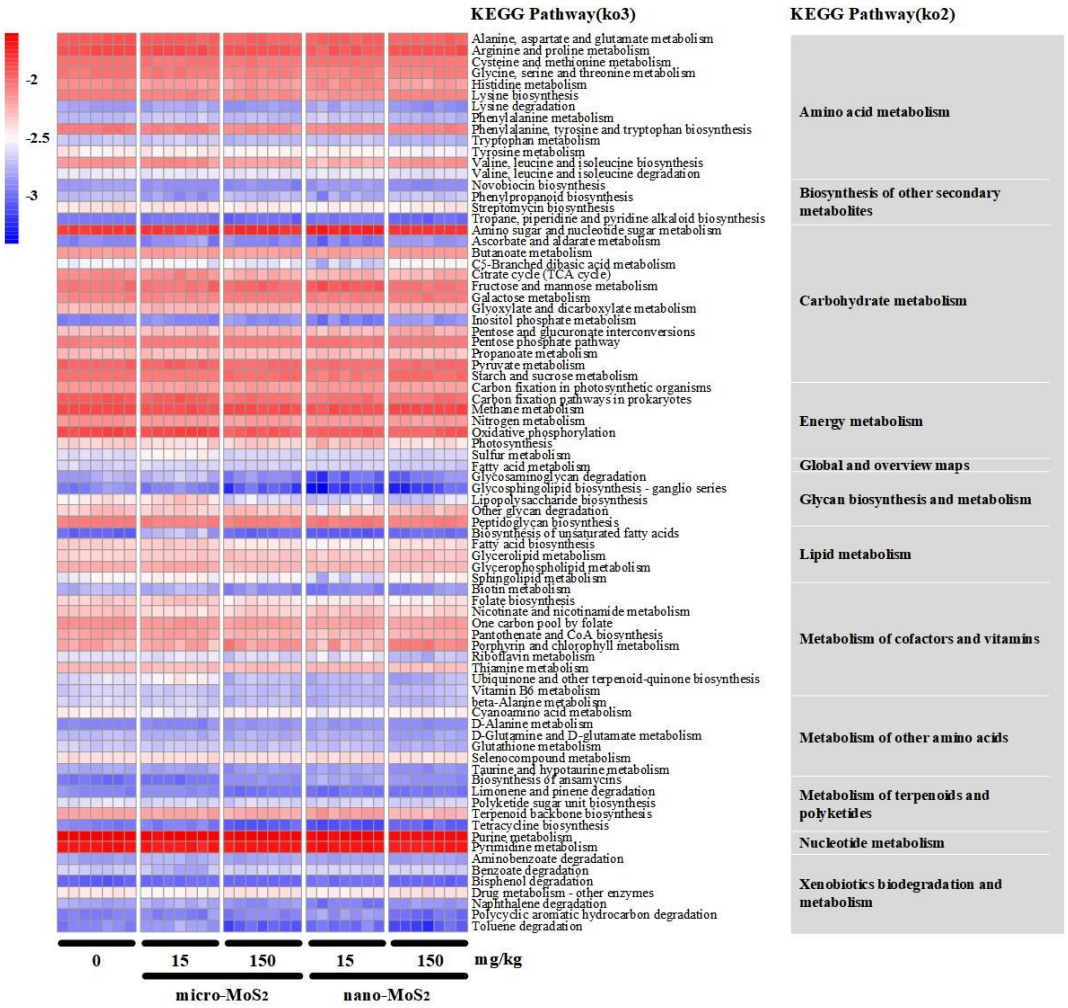

(B)

Figure S7 Influence of nano-MoS_2 and micro-MoS_2 on the metabolic pathways of intestinal microbiota of mice. (A) Small intestine; (B) Large intestine. The KEGG pathways were predicted using PICRUSt software based on their microbial community.

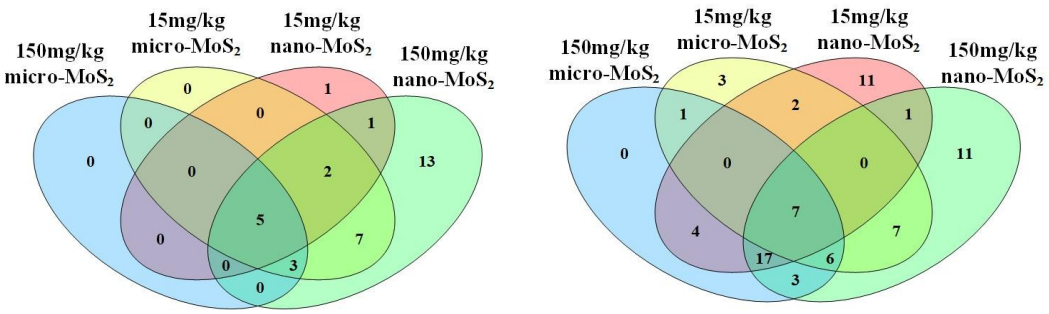

(A) (B)

Figure S8 Comparison of the predicted microbial functions in the intestine after nano-MoS_2 and micro-MoS_2 exposure based on the Venn diagram. (A) Small intestine; (B) Large intestine. The digit indicates the number of predicted KEGG pathways. The KEGG pathways were predicted using PICRUSt software.

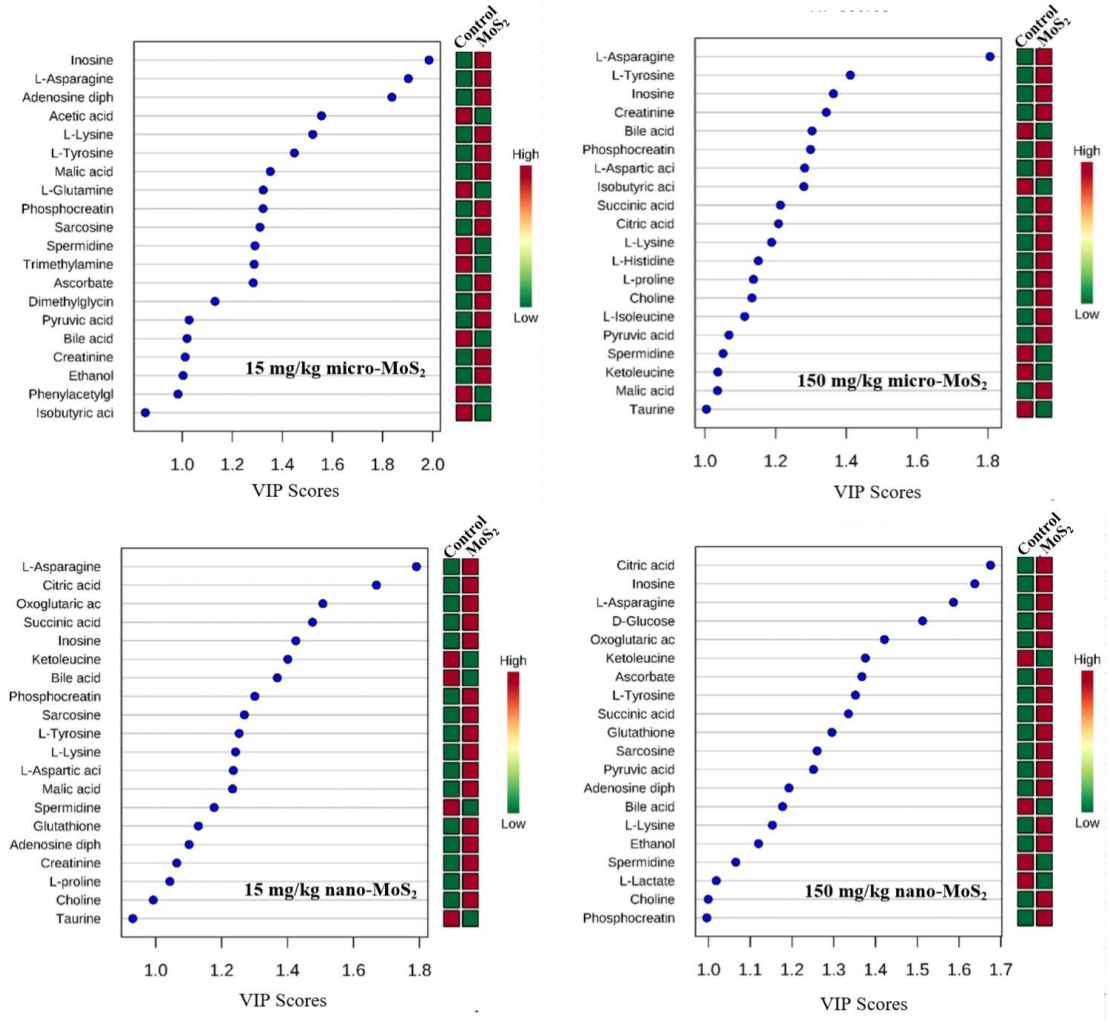

(A)

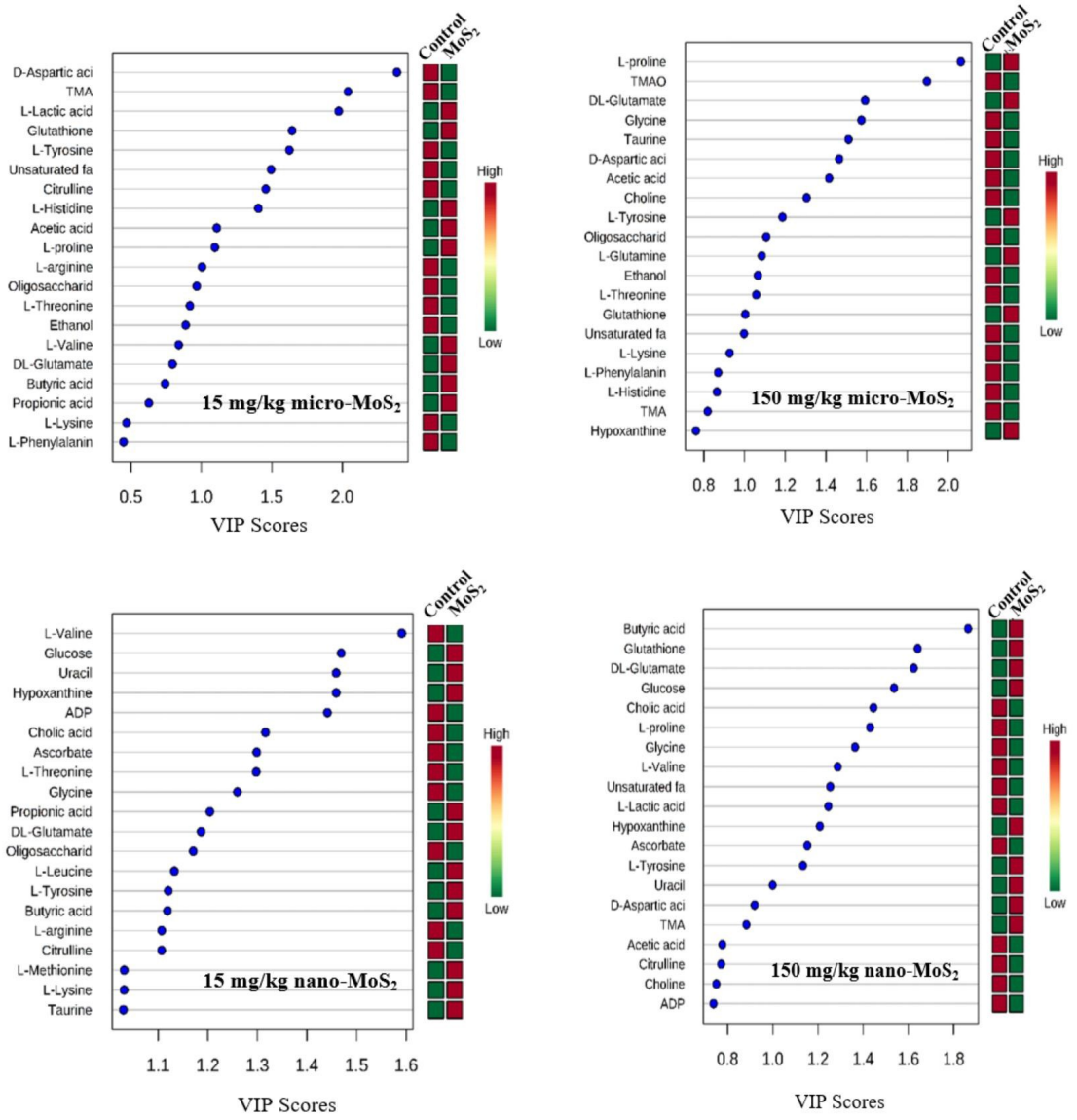

(B)

Figure S9 Metabolic profiles in the intestinal microbiota after nano-MoS_2 and micro-MoS_2 exposure. (A) Microbiota in the small intestine; (B) Microbiota in the large intestine. A total of 20 metabolites were identified based on the cumulative variable importance in the projection (VIP) value of each metabolite, which was determined using VIP analysis of MetaboAnalyst 3.0.

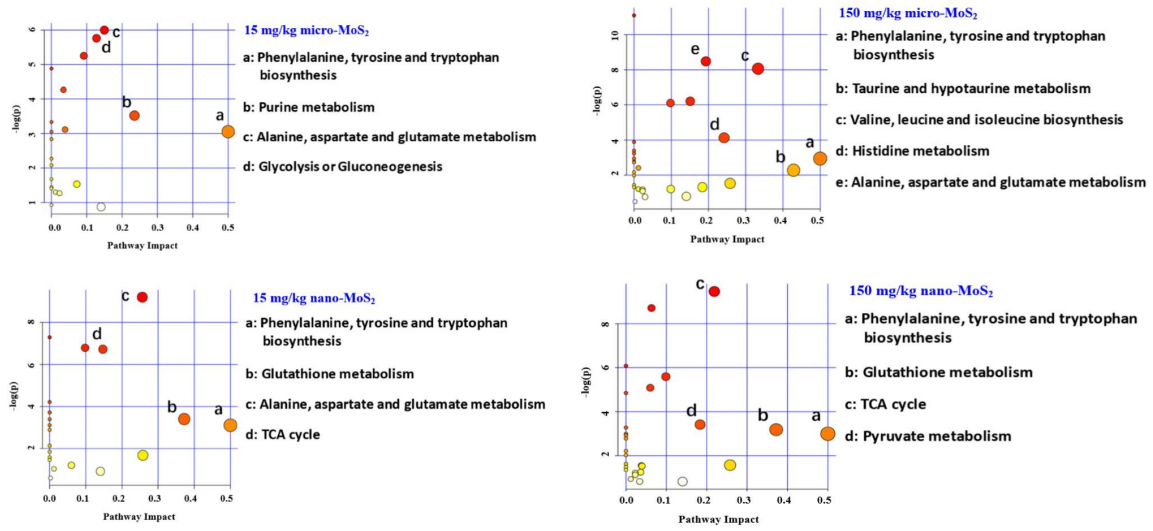

(A)

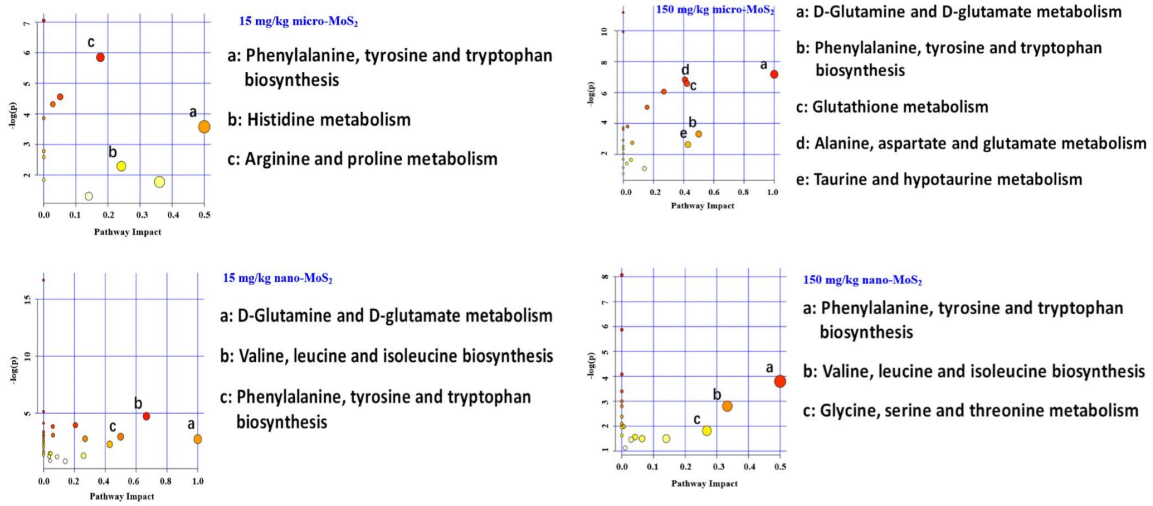

(B)

Figure S10 Influence of nano-MoS_2 and micro-MoS_2 on the metabolic pathways in the small and large intestinal microbiota of mice. (A) Small intestine; (B) Large intestine. The metabolic pathways were determined using MetaboAnalyst 3.0.

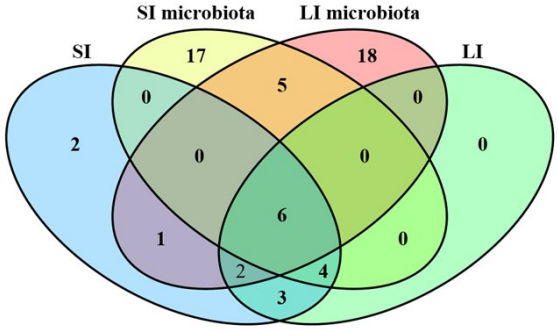

Figure S11 Correlation of the microbial-host cometabolites in the small intestine (SI) and large intestine (LI) after the MoS_2 treatment groups. The digit indicates the number of cometabolites.